lajss.org
Latin American Journal of Solids and Structures
www.lajss.org

Artificial-Intelligence-Driven Prediction of Load-Carrying Capacity of ECC-Strengthened Reinforced Concrete Beams Using Dense Learning Machine

Ahmet Tuken[a] 0000-0002-3144-4590, Yassir M. Abbas[b*] 0000-0003-2451-4770, and Nadeem A. Siddiqui[c] 0000-0002-1181-171X

[a] Department of Civil Engineering, King Saud University, Riyadh 11421, Saudi Arabia. E-mail: atuken@ksu.edu.sa
[b] Department of Civil Engineering, King Saud University, Riyadh 11421, Saudi Arabia. E-mail: yabbas@ksu.edu.sa
[c] Department of Civil Engineering, King Saud University, Riyadh 11421, Saudi Arabia. E-mail: nadeem@ksu.edu.sa

* Corresponding author

Abstract

Ensuring the structural performance of reinforced concrete beams strengthened with engineered cementitious composites (ECC) demands a reliable prediction of their load-carrying capacity. This task is complicated by the nonlinear interactions among material properties, geometry, and applied loads. This study introduces a rigorously validated dense neural network model tailored to accurately predict the load-carrying capacity of ECC-strengthened reinforced concrete beams, and provides a powerful data-driven tool for advanced structural design. A comprehensive database was assembled from published experimental programs and high-fidelity numerical simulations, which includes diverse beam geometries, reinforcement ratios, and ECC layer configurations. Among a suite of machine-learning techniques, the optimized dense neural network achieved superior predictive performance (R^2 = 0.975, mean absolute error = 14.544, root mean squared error = 18.190), which outperforms linear, tree-based, and other nonlinear models. Sensitivity analysis revealed beam depth and ECC tensile strength as dominant drivers of load-carrying capacity, while ECC layer thickness exerted a comparatively minor influence. Importantly, the inherent strain-hardening capacity of ECC was shown to markedly enhance ductility, energy dissipation, and seismic resilience. These findings highlight the potential of artificial-intelligence-based approaches to restructure the design of ECC-strengthened reinforced concrete beams, inform performance-based seismic design, and guide the next generation of robust, high-performance concrete infrastructure.

Keywords
ECC-strengthened beams, dense neural network, engineered cementitious composites, beam strengthening, infrastructure rehabilitation.

1 INTRODUCTION

1.1. Background

Reinforced concrete (RC) beams are among the most widely used structural elements in buildings, bridges, and infrastructure systems. However, during their service life, these structural members may deteriorate due to aging, corrosion, fatigue loading, environmental exposure, design deficiencies, seismic actions, and increasing service load requirements. Consequently, strengthening and rehabilitation of existing RC beams have become essential for restoring structural integrity, enhancing load-carrying capacity, improving durability, and extending service life. In recent years, engineered cementitious composites (ECC) have emerged as one of the most promising strengthening materials because of their exceptional tensile ductility, strain-hardening characteristics, superior crack control ability, and improved durability performance (Ji et al., 2023; Zhu et al., 2022). Unlike conventional cementitious materials, ECC exhibits multiple microcracking behaviors instead of localized brittle cracking, which significantly enhances structural resilience and energy absorption capacity.

The incorporation of ECC in RC beams has demonstrated substantial improvements in flexural performance, shear resistance, ductility, stiffness, crack distribution, and long-term durability. Despite these advantages, accurately predicting the load-carrying capacity of ECC-strengthened RC beams remains a major challenge because the structural response depends on highly nonlinear interactions among several influencing parameters, including material properties, reinforcement details, ECC thickness, beam geometry, bond characteristics, and loading conditions.

Traditionally, prediction of the load-carrying capacity of strengthened RC beams has relied on empirical, semi-empirical, or mechanics-based analytical models. Although these approaches provide useful insights, they often fail to fully capture the complex nonlinear behavior associated with ECC-strengthened systems. Recent developments in computational intelligence and artificial intelligence (AI) have introduced new opportunities for addressing such complex structural engineering problems. Among these approaches, machine learning (ML) techniques have demonstrated strong capability in identifying hidden nonlinear relationships from large datasets without relying on simplifying assumptions.

Dense neural networks (DNNs), a specialized class of artificial neural networks, have gained increasing attention because of their ability to process high-dimensional data and model highly nonlinear systems (Agliari et al., 2023). DNNs have shown excellent performance in predicting various structural engineering properties, including compressive strength, shear capacity, flexural resistance, and durability-related parameters. Their ability to learn complex interactions among multiple variables makes them particularly suitable for predicting the load-carrying capacity of ECC-strengthened RC beams. Nevertheless, despite the growing application of AI in structural engineering, the use of dense neural networks for predicting the structural behavior of ECC-strengthened RC beams remains relatively underexplored.

1.2. Literature Review

A considerable number of studies have investigated the structural performance of ECC-strengthened RC members and the application of machine learning methods in structural engineering. Tuken et al. (2023) developed a machine learning framework using the XGBoost algorithm for predicting the load-carrying capacity of ECC-strengthened beams. Their model was trained using data collected from more than 20 published studies comprising 217 beam specimens. The developed framework incorporated 20 input variables and achieved prediction accuracies exceeding 80%. The study identified reinforcement yield strength, ECC layer thickness, beam depth, and reinforcement area as the most influential parameters affecting load capacity. In addition, SHapley Additive exPlanations (SHAP) analysis was employed to quantify the contribution of individual parameters, and a graphical user interface was proposed for practical engineering implementation.

Ge et al. (Ge et al., 2024) evaluated the effectiveness of five machine learning algorithms, including Extreme Gradient Boosting (XGBoost), Support Vector Regression (SVR), Random Forest (RF), Multilayer Perceptron (MLP), and Extremely Randomized Trees (ERT), for predicting the bending capacity of hybrid-reinforced ECC-concrete beams. Based on a database consisting of 150 experimental specimens, XGBoost demonstrated superior predictive capability compared to other algorithms. The study further identified reinforcement ratio and fiber-reinforced polymer (FRP) bar strength as the most critical variables influencing bending capacity. To facilitate practical applications, the authors also developed a graphical user interface for engineers and researchers.

Guo et al. (Guo et al., 2024) numerically investigated the flexural-shear performance of strengthened RC beams incorporating ECC layers and FRP grids. Their findings showed that ECC layers significantly enhanced shear capacity and improved crack distribution, while FRP grids effectively reduced stress concentrations and prevented premature cracking. Furthermore, the study proposed a predictive equation for estimating shear capacity, which was validated using both numerical and experimental results.

Tabrizikahou et al. (Tabrizikahou et al., 2022) studied the strengthening of masonry shear walls using pseudoelastic Ni–Ti shape memory alloy (SMA) strips and ECC sheets subjected to quasi-static cyclic loading. The results demonstrated that the hybrid strengthening system substantially improved structural stiffness, energy dissipation, and seismic resilience. The thickness of ECC sheets and SMA strips was also found to significantly influence overall structural performance.

Wang et al. (C. Wang et al., 2023) investigated chloride penetration in ECC subjected to sustained flexural loading conditions. The study revealed that fiber bridging in ECC effectively restricted microcrack widths, thereby reducing chloride diffusion compared to conventional concrete materials. The authors further developed a binary model linking chloride diffusion coefficients with tensile stress and exposure duration, providing useful insights for the durability design of ECC-concrete structures.

Qin et al. (Qin et al., 2020) experimentally investigated the flexural behavior of RC beams strengthened using high-strength high-ductility ECC (HSHD-ECC). Seven beam specimens were tested, including one control beam and six strengthened beams with varying ECC layer thicknesses and reinforcement ratios. The results showed substantial improvements in cracking load, yielding load, and ultimate load due to ECC strengthening. Unlike conventional RC beams, the ECC-strengthened beams exhibited distributed multiple microcracks rather than localized macrocracks. The authors also proposed a simplified flexural capacity prediction method that achieved an average prediction ratio of 0.94 with a coefficient of variation of 0.03.

Zhang (Zhang, 2018) experimentally examined the behavior of ECC-strengthened RC members and proposed a prediction model for estimating load-carrying capacity. The study highlighted the significant influence of ECC layer thickness on crack development and structural performance. Validation against experimental data confirmed the effectiveness of the proposed model in estimating flexural strength.

Yuan et al. (Yuan et al., 2020) proposed a simplified constitutive model for ECC and employed finite element analysis to simulate the flexural behavior of ECC-strengthened RC beams. The numerical predictions showed strong agreement with experimental observations, confirming the reliability of the developed constitutive model. The study further evaluated the influence of ECC modulus, tensile ductility, layer thickness, and placement configuration on ultimate moment capacity, deflection response, and crack width behavior.

Qi et al. (Qi et al., 2018) developed a linear constitutive model for ECC and investigated moment-curvature relationships considering various material parameters. Their findings demonstrated that transition strain, post-cracking tensile stiffness, and strain-softening characteristics significantly influenced structural response, whereas compressive properties had comparatively minor effects. A four-point bending test program was conducted, and the modified numerical approach showed good accuracy in predicting tensile strength behavior.

Cahyati et al. (Cahyati et al., 2021) investigated the influence of ECC patch size on the repair performance of cracked RC beams. Numerical analyses performed using ABAQUS demonstrated that ECC patches significantly improved flexural load-carrying capacity compared to conventional concrete repair systems. The study further showed that patch length and depth ratios strongly affected beam stiffness and ductility, while optimized patch dimensions improved structural integrity and performance.

Recent advances in explainable artificial intelligence have also enhanced predictive modeling applications in structural engineering. Abbood et al. (Abbood, Rahman, & Abu Bakar, 2025; Abbood, Rahman, & Bakar, 2025) developed advanced machine learning frameworks for predicting the shear strength of reinforced concrete deep beams using large experimental databases and explainable AI techniques. Their studies incorporated ensemble learning algorithms, including XGBoost and CatBoost, combined with Bayesian optimization, SHAP analysis, and partial dependence plots (PDPs) to improve prediction accuracy and interpretability. The developed models demonstrated superior predictive performance compared to conventional design equations and other AI-based approaches while also identifying the influence of key geometric and material parameters on shear behavior. These studies contributed significantly to the integration of transparent and reliable AI methods into structural engineering analysis and design.

Liao et al. (Liao et al., 2021) proposed a predictive model for estimating the flexural deflection of ultra-high-strength rebar-reinforced ECC beams. The developed bilinear stress-strain model considered different reinforcement ratios and matrix materials. Experimental validation confirmed the accuracy of the model in predicting beam deflections and demonstrated that high-strength reinforcement could reduce reinforcement requirements while maintaining excellent flexural performance.

Ismail and Hassan (Ismail & Hassan, 2021) experimentally evaluated large-scale repaired normal concrete beams strengthened with fiber-reinforced cementitious composites. Both ECC and steel fiber-reinforced cementitious composites (SFRCC) were investigated for strengthening the tension and compression zones of RC beams. The results showed that beams repaired using SFRCC exhibited superior crack control and energy absorption capacity compared to ECC-repaired beams, indicating enhanced durability and structural performance.

Overall, previous studies have confirmed the significant potential of ECC materials and machine learning techniques in improving structural performance prediction and strengthening design. However, important challenges and research gaps remain.

1.3. Research Gap

Despite the substantial progress achieved in ECC strengthening systems and machine learning-based predictive modeling, several important limitations remain unresolved in the existing literature. Many previous studies focused primarily on experimental investigations or conventional analytical models for predicting flexural or shear behavior separately. Although these methods provide valuable understanding of structural response, they often require simplifying assumptions and may not fully capture the highly nonlinear interactions among material properties, geometric characteristics, reinforcement details, and ECC strengthening parameters.

Existing machine learning studies have mainly employed ensemble learning algorithms such as XGBoost, Random Forest, and CatBoost. While these approaches have demonstrated good predictive capability, the application of dense neural networks for predicting the load-carrying capacity of ECC-strengthened RC beams remains limited. Dense neural networks possess superior capability in extracting complex nonlinear relationships from large datasets, yet their potential in this particular structural engineering application has not been comprehensively explored.

In addition, previous investigations have generally concentrated on overall prediction accuracy without thoroughly examining the relative influence of key ECC parameters under different concrete strength categories. Limited studies have investigated the effects of ECC tensile strength, ultimate tensile strain, and ECC layer thickness on the load-carrying capacity of both normal-strength and high-strength RC beams. Furthermore, there remains a lack of comprehensive AI-based frameworks capable of combining accurate prediction, sensitivity analysis, and parametric evaluation within a unified modeling approach.

1.4. Objectives and Novelty

The primary objective of this study is to develop a robust dense neural network-based framework for accurately predicting the load-carrying capacity of reinforced concrete beams strengthened with ECC. To accomplish this objective, a comprehensive experimental database is compiled from previously published studies, incorporating key input parameters related to beam geometry, reinforcement properties, material characteristics, and ECC strengthening configurations.

The specific objectives of this study are summarized as follows:

1. To develop a comprehensive database of ECC-strengthened RC beams by collecting and organizing experimental data from the literature.
2. To identify the most relevant input parameters influencing the load-carrying capacity of ECC-strengthened RC beams.
3. To design, train, and optimize different machine learning models, particularly dense neural networks, for capturing the nonlinear structural behavior of ECC-strengthened beams.
4. To evaluate the predictive performance of the developed models by comparing predicted results with experimental observations.
5. To conduct detailed sensitivity analyses for both normal-strength and high-strength concrete beams.
6. To investigate the influence of ECC tensile strength, ultimate tensile strain, and ECC thickness on the load-carrying capacity of strengthened beams.
7. To provide an efficient predictive framework that can support structural design and strengthening applications.

The novelty of this research lies in the application of dense neural networks to predict the load-carrying capacity of ECC-strengthened RC beams using a large experimental database and extensive parametric evaluation. Unlike conventional empirical models and previously developed ML frameworks, the proposed approach aims to capture complex nonlinear interactions more effectively while also providing systematic sensitivity analyses for different strengthening scenarios and concrete strength categories. The study, therefore, combines advanced AI modeling with practical structural engineering applications in a unified framework.

1.5. Theoretical and Practical Contribution

This study provides important theoretical contributions by advancing the application of artificial intelligence and dense neural network modeling in structural engineering. The proposed framework improves understanding of the nonlinear relationships among ECC material properties, beam geometry, reinforcement characteristics, and strengthening configurations affecting the load-carrying capacity of ECC-strengthened RC beams. The sensitivity analyses conducted in this study also contribute to identifying the relative importance of critical parameters governing structural performance.

From a practical perspective, the developed predictive model offers engineers and researchers a reliable and efficient tool for estimating the load- carrying capacity of ECC-strengthened RC beams without relying solely on expensive and time-consuming experimental testing or simplified empirical equations. The proposed framework can support the design, optimization, assessment, and rehabilitation of strengthened RC structures while improving prediction accuracy and structural safety. Moreover, the findings of this study may encourage wider implementation of ECC-based strengthening systems and AI-assisted design approaches in modern infrastructure engineering applications.

2 DATABASE CONSTRUCTION

2.1. The variables of the study

The type of fibers (e.g., synthetic/hybrid synthetic/hybrid metallic/hybrid synthetic-metallic) used in the ECC and the type of test (three points/four points) were not considered as variables in this study, since their impact on the load capacity of the ECC strengthened beams was found to be insignificant by the authors (Tuken et al., 2023). In the present study, 14 variables were considered, as shown in Table 1.

Table 1. Input and Output variables used in the study.

Variable	Type	Definition	Unit	No of data	
				Present	Missing
CS	Input	Compressive strength of the existing concrete	MPa	283	——
RI	Input	Reinforcement index of fibers used in the ECC [Eq. (1)].	% (vol.)	242	41
TS	Input	Tensile strength of the ECC	MPa	241	42
US	Input	Ultimate strain of the ECC	%	211	72
WB	Input	Width of the beam	mm	283	——
DB	Input	Depth of the beam	mm	283	——
SL	Input	Span length	mm	283	——
SD	Input	Shear span-to-depth ratio	——	238	45
SR	Input	Shear reinforcement ratio effective in shear ($A_{sv}/(bS_v)$)	%	212	71
YS	Input	Yield strength of the stirrups	MPa	199	84
AS	Input	Cross-sectional area of longitudinal reinforcement in the main beam	mm^2	210	73
YB	Input	Yield strength of the main beam's steel reinforcement	MPa	194	89
TC	Input	ECC layer's thickness	mm	283	——
LC	Output	Load-carrying capacity	kN	283	——

In this table, the reinforcing index was defined as

$$\mathrm{RI} = \sum V_f \, L_f / d_f \tag{1}$$

Where, RI is a reinforcing index, d_f is fiber diameter (mm), V_f is the fibers' volume fraction (%), and L_f is the fiber length (mm).

To account for the effects of specimen size and geometry, Table 2 was used, following the procedure outlined in Naaman & Wille (Naaman & Wille, 2010) and Skazlic et al. (Skazlic M et al., 2008) for modification factors, with a 100 mm cube as the reference. The dataset was split into 80% for training and 20% for testing. Furthermore, the actual tensile strength (f_t') of concrete was estimated as 90% of the split tensile strength, in accordance with the fib Model Code for Concrete Structures (fib Model Code for Concrete Structures, 2010). Additionally, f_t' was determined using Eq. 2, based on the French code in (AFGC, 2002), where f_b' represents the flexural strength of concrete and h denotes the height of the tested prism.

$$f_t' = \left(\frac{0.8h^{0.7}}{1 + 0.8h^{0.7}}\right) f_b' \quad (2)$$

Table 2. Coefficient for size and type effects in data processing

Specimen	Type	Cylinder		Cube
	Size	100×200 mm	150×300 mm	150 mm
Coefficient		1.020	1.063	1.119

2.2. Addressing missing data

To handle missing data effectively, it is important to consider the variables' characteristics, the amount of missing data, and the type of missingness (Emmanuel et al., 2021). In this study, the variables with missing data were classified into three categories: (i) MCAR (Missing Completely at Random): When the missing data is unrelated to other variables, simple imputation methods are often sufficient. (ii) MAR (Missing at Random): When the missingness is dependent on observed data, more advanced imputation techniques, such as regression or k-nearest neighbors (KNN), are appropriate. (iii) MNAR (Missing Not at Random): Imputation for MNAR data relies heavily on domain-specific knowledge.

To quantify data missingness, it was categorized as low (<30%), moderate (30–50%), and high (>50%). For addressing missing values in specific variables, a customized imputation strategy was employed, tailored to each feature's characteristics. Missing values in the reinforcement index of fibers used in the ECC variable were replaced using the column mean, ensuring the preservation of central tendencies, particularly in normally distributed data. Similarly, for the tensile strength of the ECC variable, the median was used to account for potential outliers, offering a robust measure of central tendency. Although mean imputation was initially considered for the shear span-to-depth ratio, it was excluded in favor of more domain-specific techniques. This imputation strategy was implemented using the “fill blanks” method, effectively resolving missing data while maintaining the dataset's structural integrity for subsequent analyses.

For addressing moderate missing data, K-Nearest Neighbors (KNN) imputation was applied to maintain dataset completeness while preserving statistical relationships. This method specifically targeted key variables such as shear span-to-depth ratio, shear reinforcement ratio effective in shear, and ultimate strain of the ECC. Using the KNN Imputer module from scikit-learn, the number of neighbors was optimized (n_neighbors=5) to balance accuracy and computational efficiency. The algorithm identified the five closest neighbors for each missing value and imputed the missing entries using their mean. This approach ensured precise imputation without altering the integrity of other dataset columns. The imputed data was then validated through inspection, confirming that missing values were resolved without inconsistencies. KNN imputation was selected for its ability to leverage multivariate relationships, facilitating robust data preprocessing for subsequent machine learning and statistical analyses. By utilizing a structured and reproducible method, this approach mitigated the effects of missing data, improving the reliability of research outcomes.

For high levels of missing data, an iterative imputation approach was adopted using the Iterative Imputer from the scikit-learn library, focusing on the columns: yield strength of the stirrups, cross-sectional area of longitudinal reinforcement in the main beam, and yield strength of the main beam's steel reinforcement. This method employs multivariate imputation techniques, iteratively predicting missing values based on other features in the dataset. To ensure reproducibility, the Iterative Imputer was configured with a fixed random state. The algorithm performed a fit-and-transform operation on the selected columns, imputing missing values while preserving the integrity of the remaining dataset. Post-imputation, the dataset was reviewed to verify accuracy and consistency. This iterative method was chosen for its ability to generate precise, context-aware imputations, significantly enhancing the dataset's reliability for subsequent analyses.

2.3. Data exploration and preprocessing

Data exploration helps in identifying patterns, missing values, and outliers, while preprocessing ensures that the data is clean, consistent, and ready for training machine learning models. Proper preprocessing can significantly improve model performance. Table 3 shows the statistical values of all the input and output variables used in the present study. Figure 1 shows the range of input/output data values for all the variables considered in the present study. The correlation

between the various variables is shown in Figure 2, which shows that there is a strong correlation between the variables.

Table 3. Comprehensive statistical overview of the input and output variables.

Statistical Metric	Variable													
	CS	RI	TS	US	WB	DB	SL	SD	SR	YS	AS	YB	TC	LC
min	20.4	0.0	1.940	0.010	100.0	100.0	300.0	0.860	0.108	240.0	100.5	276.0	0.0	1.8
max	61.5	20.0	14.300	4.800	225.0	350.0	2400.0	4.575	2.094	609.0	981.7	924.0	300.0	668.0
range	41.1	20.0	12.360	4.790	125.0	250.0	2100.0	3.715	1.987	369.0	881.2	648.0	300.0	666.2
mean	39.1	6.2	5.868	2.453	151.1	206.7	1469.2	2.348	0.834	361.8	415.8	457.3	54.1	110.0
StdDev	11.0	5.2	2.587	1.369	38.4	76.8	525.7	0.724	0.626	86.6	245.1	105.0	64.8	102.2
Median	36.3	6.0	4.920	2.960	150.0	200.0	1650.0	2.330	0.670	361.8	402.1	456.5	40.0	93.6
Mode	39.5	6.2	4.920	4.000	150.0	300.0	1800.0	2.650	2.094	361.8	415.8	457.3	0.0	2.4
Q1	32.0	2.1	4.000	1.500	115.0	150.0	1200.0	2.000	0.390	329.0	226.2	400.0	20.0	37.7
Q3	40.1	6.7	8.000	3.490	200.0	300.0	1800.0	2.650	1.005	406.0	415.8	467.0	60.0	146.0
Skewness	0.6	1.1	0.925	–0.159	0.2	0.1	–0.8	0.740	1.160	0.7	1.2	2.7	2.2	2.0
Kurtosis	–0.6	0.8	–0.074	–1.030	–1.0	–1.4	–0.2	1.566	0.054	0.9	0.5	10.1	4.9	6.8

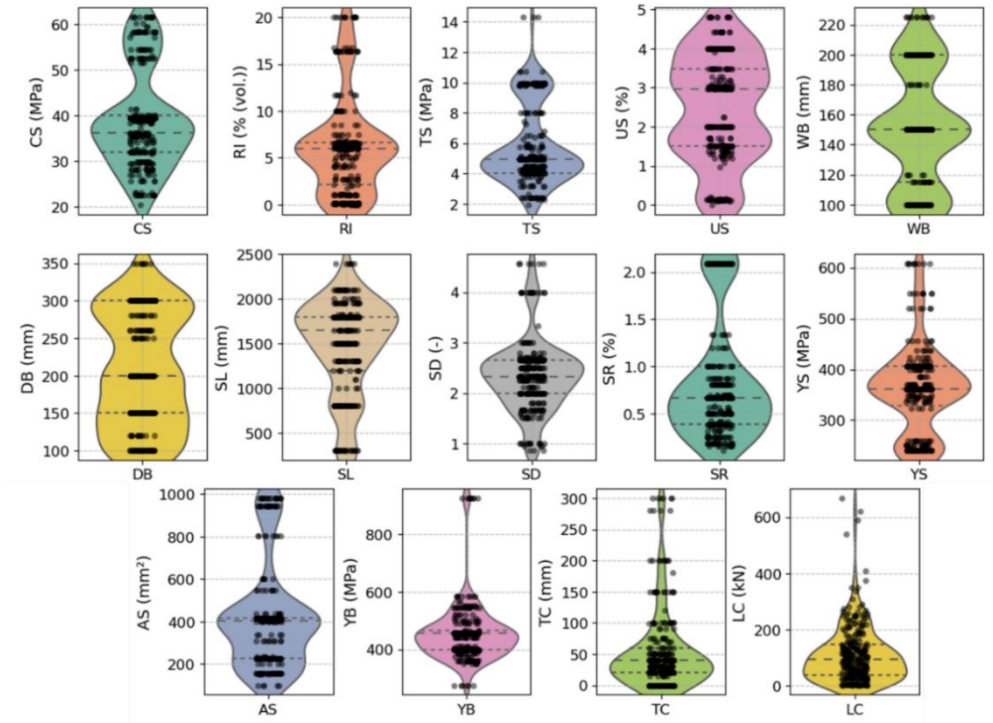

Figure 1. Violin plots illustrating the distribution patterns of the variables after mutation.

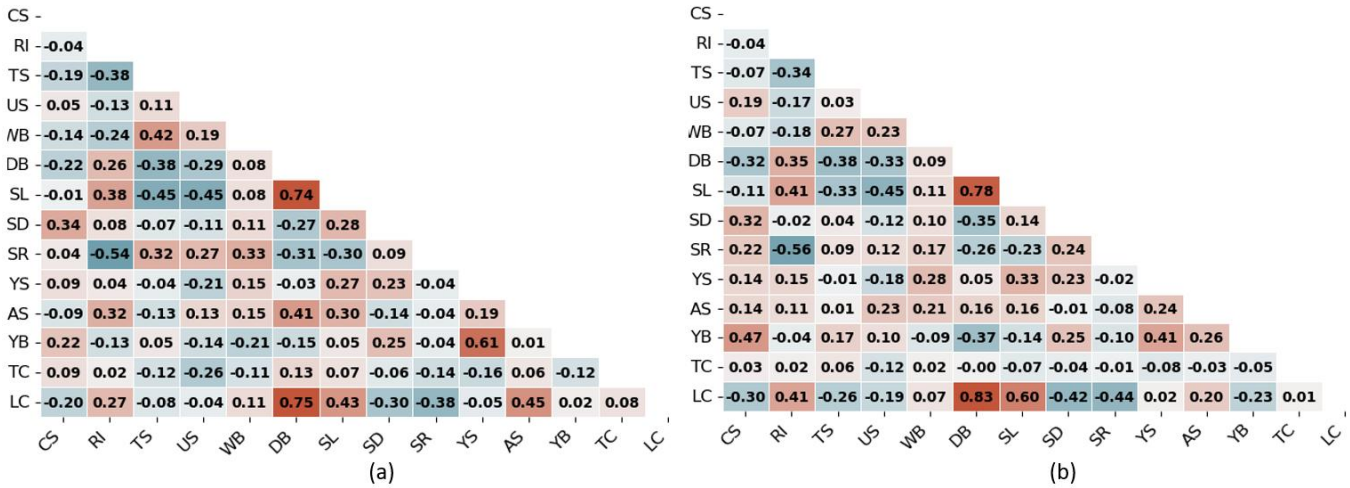

Figure 2. Pairwise relationships among variables via: (a) Pearson's, and (b) Spearman's correlation coefficient.

Table 4. List of detected outliers.

CS	RI	TS	US	WB	DB	SL	SD	SR	YS	AS	YB	TC	LC
23.2	5.0	10.7	1.7	150	200	1500	2.25	0.42	362	402.1	362	0	23.6
36.0	10.0	10.0	3.0	180	350	1500	1.50	0.16	335	549.8	585	15	540.8
36.0	6.7	10.0	3.0	180	350	1500	1.50	0.16	335	549.8	585	15	590.3
36.0	6.7	10.0	3.0	180	350	1500	1.50	0.16	335	549.8	585	15	619.8
36.0	6.7	10.0	3.0	180	350	1500	1.50	0.16	335	549.8	585	15	668.0
32.0	2.7	4.0	3.3	150	300	1800	2.57	2.09	259	402.1	386	20	250.0
32.0	2.7	4.0	1.4	150	300	1800	0.86	2.09	259	402.1	386	20	117.0
32.0	2.7	4.0	4.0	150	300	1800	2.63	2.09	259	981.7	374	40	350.0
22.5	1.0	9.8	2.0	150	150	300	1.00	0.25	240	226.2	400	50	58.9
22.5	1.0	9.8	2.0	150	150	300	1.00	0.25	240	226.2	400	0	26.6
22.5	1.0	9.8	2.0	150	150	300	1.00	0.25	240	226.2	400	75	57.6
39.9	6.7	4.9	2.0	200	300	2100	2.33	0.52	400	603.2	400	300	263.2

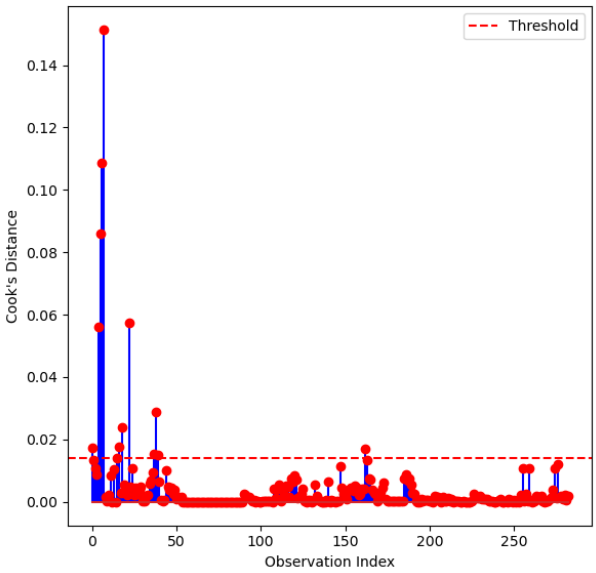

Figure 3. Cook's distance for identifying outliers.

A total of 12 outliers were excluded based on Cook's distance analysis (Table 4 and Figure 3). Thus, the size of the database after preprocessing is 271. These 271 data were obtained from 32 sources (Afefy et al., 2015; Ali & Khan, 2017; Arulanandam et al., 2022; Asgari et al., 2019; Awad et al., 2022; Basha et al., 2019; Daugevičius et al., 2016; Ge et al., 2019; Hemmati et al., 2014; Hussein et al., 2012; Ibrahim, 2021; Kamal et al., 2008; Khalil et al., 2017; M. I. Khan et al., 2021; S. W. Khan et al., 2023; A. Krishnaraja & Kandasamy, 2017; A. R. Krishnaraja & Kandasamy, 2018; Kumar & Karthikeyan, 2016; Li et al., 2009; Luković et al., 2019; Nguyen et al., 2021; O. El-Mahdy et al., 2022; Rizo-Maestre et al., 2022; Saranya & Doraikkannan, 2018; Shanour et al., 2018; Shriram et al., 2018; Siva & Pankaj, n.d.; Umer Sial & Iqbal Khan, 2018; G. Wang et al., 2019, 2020; Wei et al., 2020; Yuan et al., 2020). Figure 4 displays the distribution plots for selected model features and target variables following the removal of outliers.

The data were eventually processed via z-score normalization. The goal of this process is to transform the dataset such that each feature has a mean of 0 and a standard deviation of 1, ensuring comparability across features with different scales. First, the mean and standard deviation for each feature in the dataset are calculated. Subsequently, the mean is subtracted from each feature, centering the data around zero. Finally, each feature is divided by its standard deviation, scaling the data to unit variance. This normalization technique is crucial for machine learning models sensitive to the scale of input data, such as those relying on distance metrics or gradient-based optimization methods.

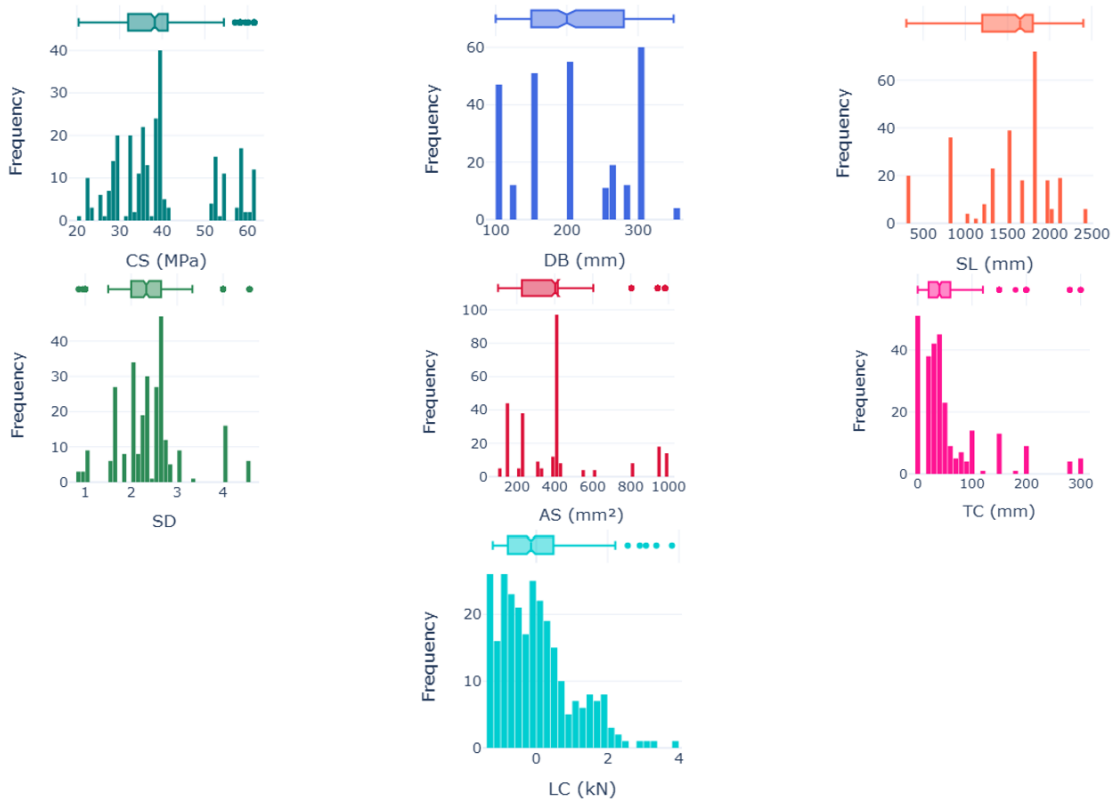

Figure 4. Distribution plot for some of the model features and labels

3 METHODOLOGY

To prepare the dataset for training and evaluation, a systematic data-splitting strategy was implemented using the train_test_split function from the scikit-learn library. This method divides the dataset into training and testing subsets, ensuring that the model is trained on one portion of the data and evaluated on another to assess its generalization capabilities. Specifically, the independent variables (X) and the target variable (y) were split into training sets (X_train, y_train) and testing sets (X_test, y_test) with a 30% test size, retaining 70% of the data for training. The split was performed using a fixed random seed (random_state=8) to guarantee the reproducibility of results. This initial hold-out strategy ensured that the model was trained on a representative majority of the data while preserving a sufficiently large and completely unseen subset for an independent assessment of its generalization capability. Recognizing, however, that a single random split may introduce bias when data distributions are uneven, this procedure was complemented with 10-fold cross-validation. In this additional analysis, the dataset was partitioned into ten stratified folds so that each observation served as both training and testing data in different iterations, and the predictive metrics were averaged across folds. The cross-validated results were consistent with those from the original 70 %–30 % split, thereby confirming that the model's performance is robust and not dependent on any specific data partitioning.

To evaluate a diverse set of machine learning algorithms for regression tasks, a function was implemented to assemble and return a comprehensive collection of models. This function includes a variety of approaches, ranging from traditional linear regression to advanced ensemble techniques and neural networks. The models were organized into distinct categories based on their underlying methodologies:

i. Linear Models: These include Linear Regression, Ridge, Lasso, ElasticNet, and Bayesian Ridge, which are widely used for their simplicity and interpretability in capturing linear relationships between predictors and the target variable.

ii. Non-Linear Models: To capture more complex patterns, K-Nearest Neighbors (KNN), Decision Trees, and Support Vector Regression (SVR) were employed. These methods excel in scenarios where data relationships deviate from linearity.

iii. Ensemble Models: Recognizing the power of ensemble techniques in improving prediction accuracy, Random Forest, Extra Trees, Gradient Boosting, AdaBoost, and Bagging Regressor were included. These models aggregate the predictions of multiple base estimators to reduce variance and bias.

iv. Advanced Gradient Boosting Methods: The list features XGBoost and LightGBM, both of which are highly efficient implementations of gradient-boosting algorithms designed to handle large datasets and complex features effectively.

v. Neural Network Models: Finally, various ANN models were included, configured with a single hidden layer of 16 to 256 neurons and a maximum of 200 iterations to leverage the adaptability of neural networks in modeling intricate relationships.

This comprehensive suite of models was implemented using the scikit-learn library for most algorithms, alongside xgboost and lightgbm libraries for advanced gradient boosting. This setup's flexibility facilitates a systematic model comparison, allowing for the selection of the most effective approach based on the dataset's characteristics and research goals.

4 RESULTS AND DISCUSSION

4.1. Prediction performance of the developed machine learning models

The performance of the machine learning models mentioned in Table 5 and Figure 5 was analyzed in terms of R^2, Mean Absolute Error (MAE), Root Mean Squared Error (RMSE), and runtime. Five major categories of machine learning models were employed: (i) Linear models (i.e., Linear Regression, Ridge, Lasso, ElasticNet), (ii) Non-Linear and Distance-Based Models (i.e., KNN, SVR), (iii) Tree-Based Models (i.e., Random Forest, ExtraTrees, Gradient Boosting, AdaBoost, Bagging), (iv) Advanced Boosting Models (i.e., XGBoost, LightGBM), and (v) Artificial Neural Networks (i.e., ANN-1 to ANN-16).

Table 5. Performance of various machine learning models.

No.	Model	R^2	MAE	RMSE	Runtime (s)
0	LinearRegression	0.759	26.016	35.995	4.338
1	Ridge	0.759	26.030	35.996	0.108
2	Lasso	0.758	26.344	36.118	0.106
3	ElasticNet	0.724	30.122	38.881	0.101
4	KNN	0.878	12.504	20.479	0.148
5	SVR	0.139	54.503	73.019	0.104
6	RandomForest	0.895	9.178	16.089	1.290
7	ExtraTrees	0.877	7.411	15.481	0.809
8	GradientBoosting	0.902	9.741	16.602	0.680
9	AdaBoost	0.827	25.226	29.673	0.586
10	Bagging	0.894	9.110	16.374	0.319
11	XGBoost	0.874	7.422	15.481	0.961
12	LightGBM	0.904	10.952	18.265	5.306
13	ANN-1	0.908	17.941	25.350	0.136
14	ANN-2	0.900	18.877	26.424	0.126
15	ANN-3	0.911	16.042	25.007	0.127
16	ANN-4	0.893	17.883	27.391	0.126
17	ANN-5	0.900	17.844	26.535	0.125
18	ANN-6	0.901	16.755	26.346	0.128
19	ANN-7	0.854	21.545	32.022	0.137
20	ANN-8	0.907	16.669	25.506	0.126
21	ANN-9	0.902	16.951	26.204	0.126
22	ANN-10	0.889	17.339	27.872	0.124
23	ANN-11	0.894	17.756	27.267	0.124
24	ANN-12	0.900	17.880	26.502	0.121
25	ANN-13	0.899	18.779	26.591	0.122
26	ANN-14	0.867	19.921	30.483	0.124
27	**ANN-15**	**0.975**	**14.544**	**18.190**	**0.122**
28	ANN-16	0.881	17.759	28.835	0.126

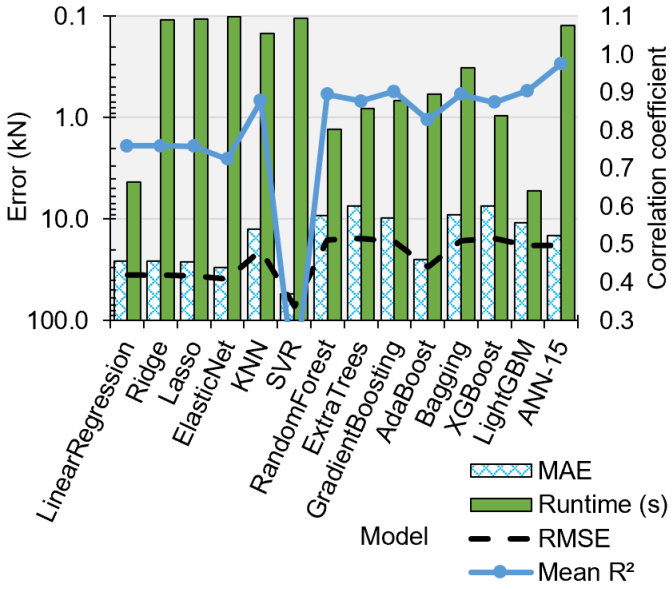

Figure 5. Visualization of performance metrics for various machine learning models.

Linear Regression provides a simple and interpretable model, but struggles with complex, non-linear patterns, often leading to lower R^2 and higher mean absolute error and root mean squared error. Ridge regression improves upon Linear Regression by adding L2 regularization and reducing overfitting, but it still struggles with feature selection. Lasso (L1 regularization) performs better when dealing with sparse data by selecting important features, often resulting in lower mean absolute error and root mean squared error. ElasticNet combines both L1 and L2 penalties, striking a balance between feature selection and regularization. These models generally have the lowest runtime but are less effective for highly non-linear data. For the present study, Table 5 shows that all the linear models except Elastic Net have similar performances. Elastic Net somehow predicts poorly compared to other linear models. The run time required for linear regression is a bit high due to the large number of variables considered in the present study. For other linear models, the number of variables does not affect the runtime much.

Among the nonlinear models, K-Nearest Neighbors (KNN) is more effective than SVR (Support Vector Regression) for capturing local patterns, as indicated in Table 5. Notably, the SVR model exhibits a markedly low R^2 (0.139), which is significantly lower than all other models. This underperformance is likely to have arisen from SVR's sensitivity to the choice of kernel function, regularization parameter, and epsilon margin. In the absence of extensive hyperparameter optimization, SVR often underfits data that are highly heterogeneous and contain complex, nonlinear interactions. The current dataset exhibits high dimensionality and pronounced variance across predictor variables, conditions that favor models capable of adaptively capturing intricate feature interactions (e.g., tree-based ensembles or dense neural networks) but challenge SVR's ability to explain an appropriate high-dimensional decision surface. Consequently, the default SVR configuration fails to exploit the latent data structure, which leads to its substantially lower R^2 compared with other model classes.

Out of the five Tree-Based Models (Random Forest, ExtraTrees, Gradient Boosting, AdaBoost, Bagging), Random Forest performs well in terms of R^2 due to its ensemble approach, reducing overfitting while maintaining interpretability. ExtraTrees provides similar or slightly better performance than Random Forest due to its more randomized feature selection. Gradient Boosting outperforms all other Tree-based models in R^2 by focusing on reducing bias. Bagging, like Random Forest, improves stability. In terms of runtime, Random Forest is slower than other models, while Bagging requires much less time, as shown in Table 5. XGBoost is one of the most popular models for structured data, delivering reasonably better R^2 with relatively lower mean absolute error and root mean squared error, due to its efficient gradient boosting mechanism. LightGBM, an optimized version of gradient boosting, tends to be almost similar to XGBoost in terms of R^2. Regarding runtime, XGBoost is much faster than LightGBM for the present data, as shown in Table 5.

ANNs excel at capturing highly complex, non-linear patterns, often achieving the highest R^2 when sufficient data is available. However, they require substantial computational resources, particularly when using dense architectures. While ANNs can achieve low mean absolute error and root mean squared error, their performance depends heavily on proper network architecture, activation functions, and optimization techniques. Unlike tree-based models, they lack interpretability, which can be a drawback in some applications. In the present study, combinations of 16 to 256 neurons with 16 steps in one hidden layer were examined, resulting in a total of 16 ANN models. The performance of these 16

ANN models is shown in Table 5. Out of these 16 models, the ANN-15 performs the best in terms of R2, mean absolute error, root mean squared error, and runtime. The performance of ANN-15 with training data and testing data is shown in Figure 6. Loss vs. iterations for the best ANN model (i.e., ANN-15) is also shown in Figure 7. It is worth noting that ANN models are faster than all the other models, as their runtime is much less compared to other machine learning models.

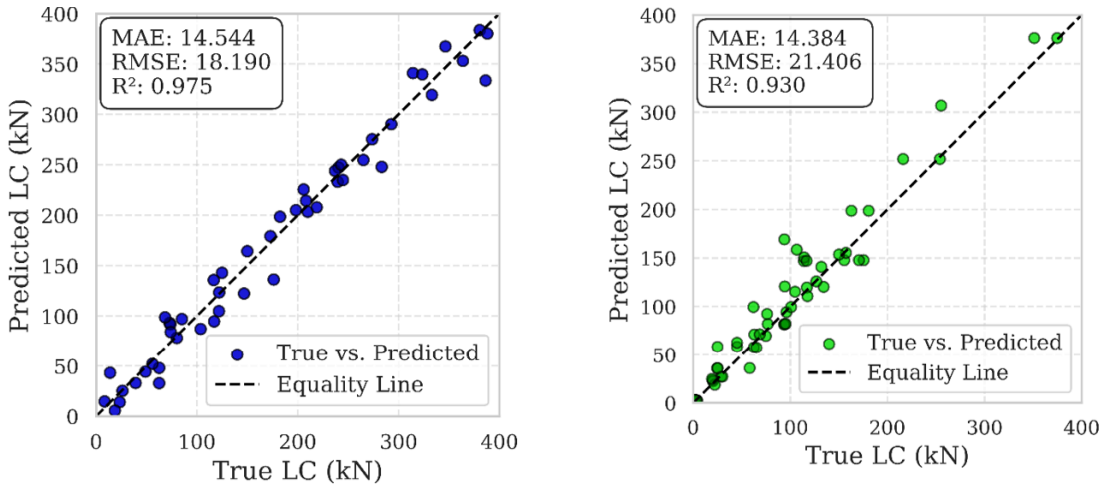

(a) (b)

Figure 6. Performance of ANN-15: (a) training data, and (b) testing data

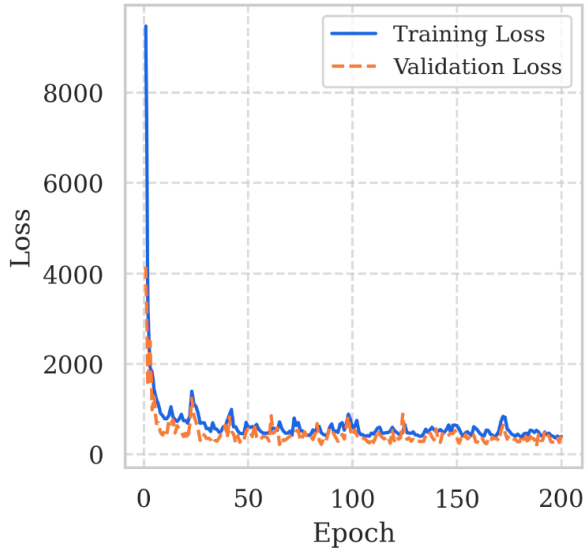

Figure 7. Loss vs. iterations for the best ANN model (i.e., ANN-15).

4.2. Mathematical representation of the best model

A single hidden-layer artificial neural network (ANN) consists of an input layer, a hidden layer, and an output layer. The network processes input features x_1,x_2,…,x_n through weighted connections w_ij, applies an activation function f(·) in the hidden layer, and then combines the hidden neuron outputs using another set of weights v_j before applying an output activation function g(·). Mathematically, the output is given by Eq. (3).

$$y = g\left(\sum_{j=1}^{m} v_j . f\left(\sum_{i=1}^{n} w_{ij} x_i + b_j\right) + c\right) \quad (3)$$

where b_j and c are biases. Common choices for f(·) include Rectified Linear Unit (ReLU), Sigmoid, or Tanh, while g(·)depends on the task (linear for regression, sigmoid for binary classification, and softmax for multiclass classification). This architecture is used in the present study for regression and classification tasks in machine learning. It is worth mentioning that the ReLU was used as an activation function in the current dense neural network. It introduces non-

linearity to the model while maintaining computational efficiency. The ReLU function was defined as: f(x)=max(0,x). This means that for any input x, ReLU returns x if it is positive and 0 if it is negative. Unlike sigmoid or tanh activations, ReLU avoids the vanishing gradient problem by allowing gradients to pass through for positive inputs, making it effective in training dense networks. Notably, the constants of the derived model in Eq. (3) are provided as supplementary material in this study.

4.3. Explanation of the optimized ANN model

4.3.1. Ranking of features

Figure 8 presents the results of the Pareto analysis, which is based on the Pareto Principle (80/20 Rule), stating that approximately 80% of the effect originates from 20% of the causes (Hossen et al., 2017). In the context of feature selection, this analysis helps identify the most influential features contributing to model performance. In this research, the significance of each input parameter (Figure 8) was evaluated based on the absolute connection weights of the input layer neurons. As depicted in Figure 8, the depth of the beam (DB) is the most significant parameter, while the thickness of the ECC layer has the least impact on the model outcome (load-carrying capacity). The analysis of absolute connection weights from the input layer of the dense neural network indicates that features such as ECC tensile strength, reinforcement ratio, and ECC layer thickness exhibit varying degrees of contribution to load-carrying capacity prediction. While parameters such as tensile strength and reinforcement ratio exhibit high importance, ECC layer thickness appears to have the lowest connection weight, despite prior studies highlighting its structural significance. Several studies highlight the impact of ECC layer properties on the structural performance of strengthened reinforced concrete beams. For instance, Guo et al. (Guo et al., 2024) report that increasing ECC tensile strength from 4 MPa to 10 MPa enhances maximum load capacity by 8.06%, while increasing ECC layer thickness from 8 mm to 20 mm results in a 14.42% increase in peak load capacity. Similarly, reinforcement configurations influence flexural performance, with higher reinforcement ratios improving bending capacity and ductility (Guo et al., 2024; Wu et al., 2024). Despite the well-documented physical role of ECC layer thickness in strengthening efficiency, its relatively low connection weight in the ANN suggests that the model assigns higher predictive value to other parameters. The influence of ECC layer thickness may be conditional rather than direct, affecting load-carrying capacity through synergistic interactions with other features. In such cases, ANN weight rankings may not fully capture their contribution, as traditional connection weight-based methods do not explicitly quantify interaction effects. The method of feature scaling applied before ANN training may also affect the relative magnitude of connection weights. If certain input variables have different normalization ranges, their weight magnitudes may not be directly comparable. Ensuring consistent scaling of all inputs can help mitigate potential distortions in feature ranking.

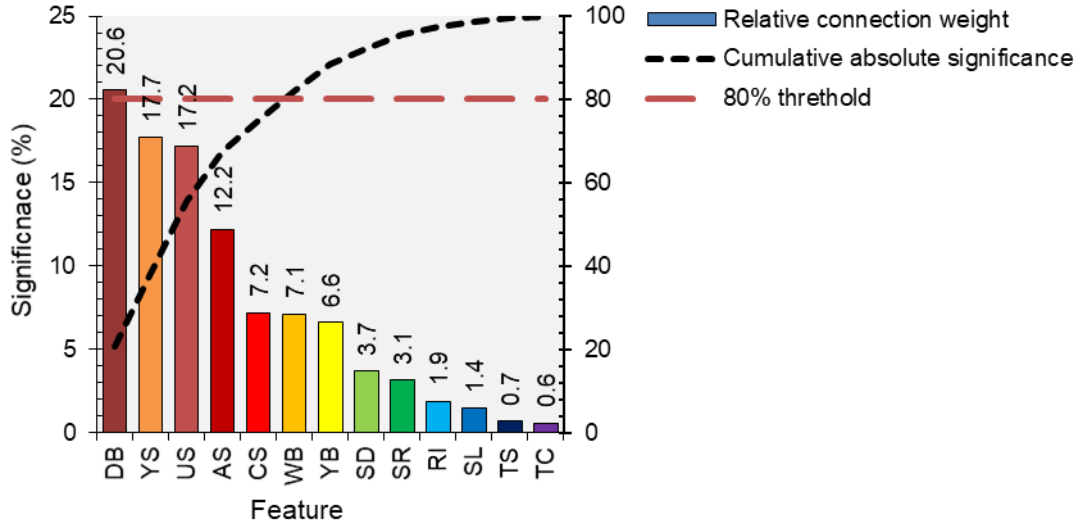

Figure 8. Pareto analysis of feature significance via the aggregated connection weights (ACW) derived from the optimized ANN model.

4.3.2. Sensitivity analysis

Figures 9 to 11 present the results of the sensitivity analysis for both normal-strength and high-strength reinforced concrete beams. This analysis examines the influence of key parameters (tensile strength, ultimate strain, and ECC thickness) on the load-carrying capacity of reinforced concrete beams strengthened with ECC, with each factor being systematically varied. The data for the reference beams used in the sensitivity analysis are detailed in Table 6.

Table 6. Overview of the reference beams used in the sensitivity analysis.

	CS	RI	TS	US	WB	DB	SL	SD	SR	YS	AS	YB	TC
	MPa	%	MPa	%	mm	mm	mm	—	%	MPa	mm^2	MPa	mm
Normal strength	28	6	2	2.5	225	300	2400	2.33	0.698	456	398.2	405.2	100
High-strength	60												

4.3.2.1 Effect of tensile strength of ECC on load-carrying capacity

In this computational study, the effect of the tensile strength of ECC on the load-carrying capacity of reinforced concrete beams strengthened with ECC has been investigated using the developed dense neural network model. The results presented in Figure 9 indicate that the tensile strength of ECC has a significant influence on the load-bearing capacity of reinforced concrete beams, which is characterized by a nonlinear trend that varies depending on the magnitude of the ECC tensile strength. The relationship between the ECC tensile strength and the load-carrying capacity of reinforced concrete beams exhibits a two-phase character. In the initial range of ECC tensile strength from approximately 2 MPa to 7 MPa, the increase in predicted load-carrying capacity is minimal and, in some cases, slightly negative. Notably, this unfavorable response highlights the governing role of steel reinforcement and interface behavior. In normal-strength reinforced concrete beams, the ultimate capacity is primarily controlled by the yielding of the longitudinal steel. Consequently, while the ECC layer's higher tensile strength markedly improves crack control, tensile stress redistribution, and ductility, it has only a limited direct influence on the ultimate load-carrying capacity once the reinforcement yields. Moreover, the superior strain-hardening and microcrack-controlling characteristics of higher-strength ECC redistribute tensile stresses more evenly, delaying the development of localized strain-energy release at the reinforcement interface. Although these mechanisms significantly enhance serviceability and post-cracking performance, they can lead to a marginal or slightly negative change in ultimate load-carrying capacity in this narrow strength interval. It is noteworthy that available experimental studies consistently attribute gains in cracking, yield, and ultimate loads to ECC's tensile behavior and crack-width control, yet none directly isolate a tensile strength increase from 2 MPa to 7 MPa. Consequently, the observed trend in the current research may be interpreted as an indicator of composite action dominated by reinforcement and interface mechanics.

Moreover, as the tensile strength exceeds 7 MPa and approaches 14.5 MPa, the influence on the load-carrying capacity becomes more pronounced, increasing at a significantly faster rate. This observation aligns with the strain-hardening behavior of ECC, where higher tensile strengths lead to a greater ability to distribute stresses, thereby improving the overall structural performance. As illustrated in Figure 9, the behavior of the load-carrying capacity as a function of ECC tensile strength highlights the importance of this parameter in improving the flexural performance of reinforced concrete beams. The increase in load-carrying capacity is modest at lower tensile strengths but becomes more substantial as the tensile strength of ECC reaches higher values. The enhancement in the flexural performance of reinforced concrete beams due to ECC is further supported by experimental studies. Similarly, Wu et al. (Wu et al., 2024) reported that the tensile strength of the ECC layer contributes to the optimization of the tensile capacity of steel reinforcement, thereby enhancing the bending capacity and overall ductility of the beam.

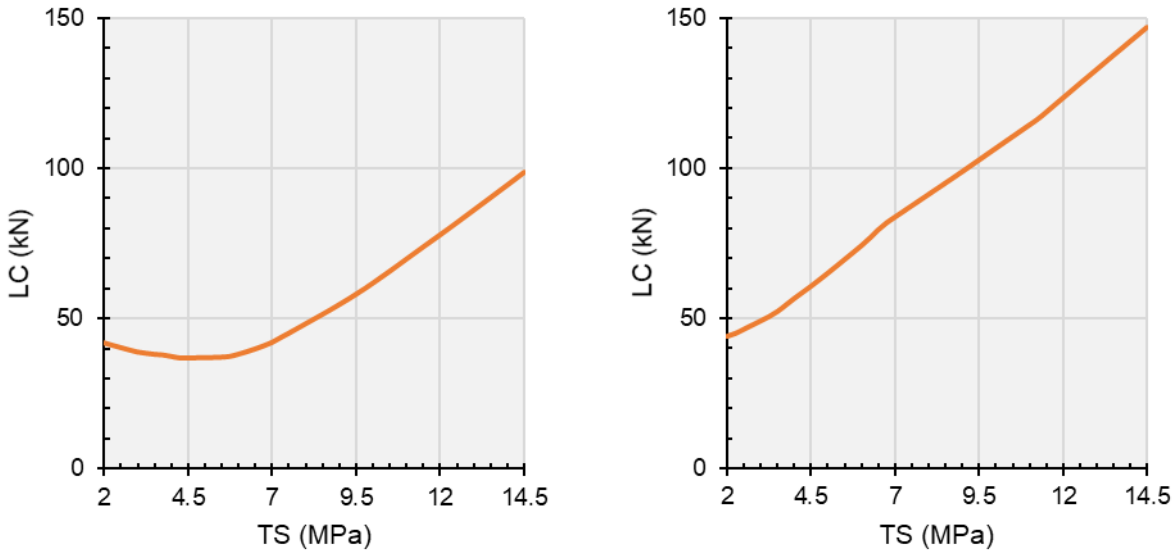

(a) (b)

Figure 9. Effect of tensile strength of ECC on the load capacity of ECC-strengthened (a) normal strength reinforced concrete beam, and (b) high-strength reinforced concrete beam.

4.3.2.2 Effect of ultimate strain of ECC on load-carrying capacity

The load-carrying capacity of reinforced concrete beams strengthened with ECC is significantly influenced by the strain capacity of the ECC material. Known for its exceptional strain-hardening characteristics, ECC can endure higher strains before failure compared to conventional concrete (Qin et al., 2020). This increased strain tolerance enhances the material's ductility and allows the beam to undergo greater deformations while preserving its load-bearing ability. As a result, ECC facilitates better redistribution of internal stresses, which delays failure and improves the overall resilience of the structure (Hu et al., 2022). In reinforced concrete beams, the enhanced strain capacity of ECC affects both the failure mode and the overall load-carrying performance. Unlike conventional concrete, which typically fails in a brittle manner upon reaching its tensile strength, ECC forms multiple fine cracks under tension, a process that improves its toughness and prevents abrupt failure. This progressive cracking behavior ensures that the beam retains significant residual load capacity even after cracks begin to form. In flexural members, such as beams, ECC's higher ultimate strain allows the section to bend more before failure, thus increasing its moment capacity. This feature is especially valuable in seismic design, where the ability to dissipate energy and exhibit high ductility is essential for the structure's safety during dynamic loading events. Furthermore, the superior bond between ECC and the reinforcement enhances the overall performance of the reinforced concrete beam. The improved load transfer between the ECC layer and the steel reinforcement ensures more efficient utilization of the reinforcement, leading to increased structural performance. By optimizing the tensile capacity of the reinforcement, ECC significantly prolongs the failure process, resulting in a more durable and effective structural system. Consequently, the load-carrying capacity of ECC-strengthened reinforced concrete beams is generally improved, owing to increased crack resistance, enhanced ductility, and superior energy dissipation.

Figure 10 depicts the influence of ECC ultimate tensile strain on the load-carrying capacity of normal- and high-strength reinforced concrete beams. For normal-strength beams, a slight decrease in the predicted load-carrying capacity is observed as the ECC ultimate strain rises when the strain capacity remains below about 2%. This negative trend may not contradict the fundamental principles of composite beam behavior. At such low ductility levels, ECC does not fully exhibit its distinctive strain-hardening and multiple-microcracking characteristics and therefore behaves more like a brittle, high-strength mortar. The resulting microcrack pattern provides less effective tensile stress redistribution and may slightly reduce the bond efficiency at the steel-matrix interface before reinforcement yielding, which leads certain data-driven models to capture a marginal decline in load-carrying capacity. Once the ECC ultimate strain exceeds roughly 2–2.5%, its characteristic high-ductility response is fully mobilized, and the load-carrying capacity increases as expected: experimental studies have reported ultimate load gains ranging from about 1.5% to 7.5% and yield-load improvements of 11–19% for ECC layers with 3–5% ultimate strain, and ultimate load rises of 6.3–10.8% with yield-load increases of 18.4–43.1% for ECC with ≈2.5% strain capacity. These findings align with other reports of significant enhancements in flexural performance when ECC exhibits ultimate strains beyond 2%. Consequently, the model-predicted decline in load-

carrying capacity below 2% strain should be interpreted as the influence of limited ECC ductility and early microcrack development rather than as a contradiction of established composite action.

Additionally, as the ultimate strain increases, the influence on load-carrying capacity becomes nearly identical for both types of beams, underscoring the crucial role of ECC's strain-hardening behavior in enhancing beam performance at elevated strain levels. Overall, incorporating ECC into reinforced concrete beams leads to substantial improvements in load-carrying capacity, primarily by increasing strain capacity, ductility, and toughness. The performance benefits of ECC can be further optimized by carefully considering factors such as the thickness and configuration of the ECC layer and the type of reinforcement used. These findings offer valuable guidance for designing and implementing ECC-strengthened reinforced concrete beams, providing potential solutions to improve the safety and performance of structures exposed to extreme loading conditions.

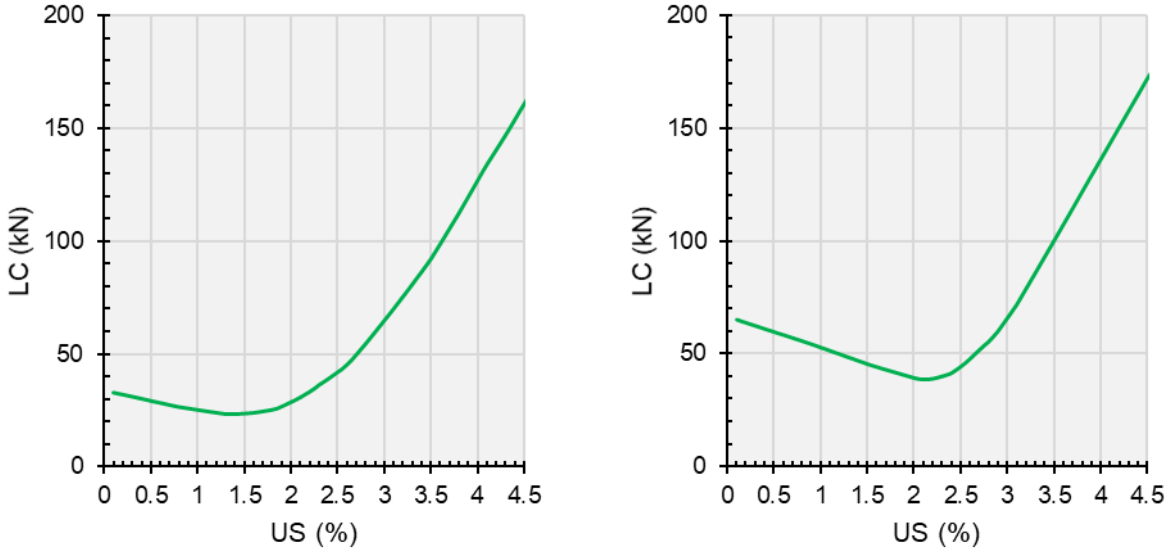

Figure 10. Effect of ultimate strain of ECC on the load capacity of ECC-strengthened (a) normal strength reinforced concrete beam, and (b) high-strength reinforced concrete beam.

4.3.2.3 Effect of the thickness of ECC on load-carrying capacity

Figure 11 depicts the influence of ECC layer thickness on the load-carrying capacity of reinforced concrete beams reinforced with ECC. The data reveal a clear trend, where increasing the thickness of the ECC layer results in a corresponding enhancement in the load-carrying capacity of the reinforced beams, showing an almost linear relationship. This improvement can be attributed to several factors intrinsic to the mechanical properties of ECC. As the ECC layer becomes thicker, the flexural stiffness of the reinforced concrete beam increases, leading to a higher moment capacity (Liu et al., 2023). Additionally, the extra tensile resistance provided by the ECC in tension zones helps delay crack initiation and reduces crack width, thereby improving the overall durability of the structure. In seismic scenarios, a thicker ECC layer proves particularly advantageous, as it enhances the beam's energy dissipation capacity, reducing the effects of dynamic loads. Furthermore, the increased thickness of the ECC layer strengthens the shear resistance of the beam (Hu et al., 2022). This is especially beneficial in beams with insufficient shear reinforcement, as the added ECC thickness improves crack bridging and shear transfer, preventing the sudden shear failure often observed in conventionally reinforced beams. The inherent ductility of ECC allows it to undergo significant deformation prior to failure, enabling the beam to support greater loads and delay catastrophic collapse. However, the relationship between ECC thickness and load-carrying capacity is not linear. As Figure 11 illustrates, the rate of increase in load-carrying capacity diminishes beyond a certain threshold of ECC thickness. This suggests the presence of an optimal ECC layer thickness, beyond which further increases may not lead to proportionally greater improvements. The addition of ECC layers not only boosts the load-carrying capacity of reinforced concrete beams but also enhances their ductility and crack control, especially in over-reinforced beams, where ECC optimizes the tensile strength of steel bars and enhances the bending capacity (Wu et al., 2024). Furthermore, ECC reduces the brittleness of reinforced concrete beams by distributing cracks more uniformly, as demonstrated in beams reinforced with high-strength steel strand mesh and ECC (Zhao et al., 2024).

While the benefits of ECC in enhancing the load-carrying capacity of reinforced concrete beams are well-documented, it is crucial to consider practical concerns regarding the thickness of the ECC layer. The added weight and cost associated with thicker ECC layers may not always be justified by performance improvements, particularly in

applications where weight constraints are critical. Additionally, the effectiveness of the ECC strengthening technique is highly dependent on the bond quality between the ECC and the underlying concrete. Poor bonding can undermine the benefits of ECC, particularly in harsh environments or under high-loading conditions. Therefore, determining the optimal ECC thickness requires a thorough evaluation of the specific structural needs, environmental conditions, and cost-effectiveness.

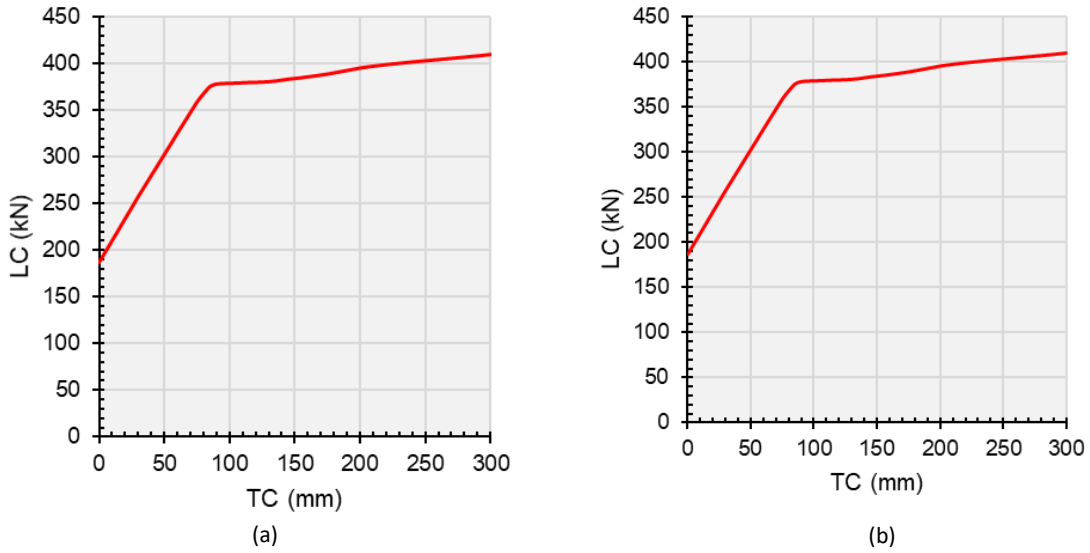

Figure 11. Effect of thickness of ECC on the load capacity of ECC-strengthened (a) normal strength reinforced concrete beam, and (b) high-strength reinforced concrete beam.

5 CONCLUSIONS, LIMITATIONS, AND FUTURE DIRECTIONS

This research presents the development of a highly accurate dense neural network model for predicting the load-carrying capacity of reinforced concrete beams strengthened with ECC. A comprehensive dataset was curated and preprocessed, incorporating experimental data and numerical simulations from previously published studies and validated computational models. The scope of the study is focused on reinforced concrete beams with ECC layers, encompassing various geometric configurations, reinforcement ratios, and ECC thicknesses. The dense neural network model was trained using supervised learning techniques, employing a systematic training-validation framework to enhance its predictive performance. The findings of this study lead to the following conclusions:

(i) ANN-15 demonstrates the best performance, achieving the highest R^2 (0.975), and the lowest mean absolute error (14.544) and root mean squared error (18.190), with a competitive runtime (0.122s). Among linear models, Lasso outperforms others with the lowest mean absolute error and root mean squared error, but all linear models underperform compared to non-linear and tree-based models. Gradient Boosting achieves the highest R^2 (0.902) among tree-based models, followed by Random Forest (0.895) and ExtraTrees (0.877). XGBoost and LightGBM perform similarly, with XGBoost being faster in runtime. KNN excels among non-linear models with an R^2 of 0.878, outperforming SVR (R^2 = 0.139). ANN models generally deliver superior accuracy but require considerable computational resources, especially when using dense architectures.

(ii) Beam depth (DB) is identified as the most significant parameter, while ECC layer thickness has the least impact on model predictions, as shown by the Pareto analysis of absolute connection weights. Tensile strength and reinforcement ratio exhibit high importance, influencing load-carrying capacity prediction significantly. The low connection weight of the ECC layer thickness suggests its influence may be conditional, potentially interacting with other features. Feature scaling prior to ANN training could distort the relative importance of features, affecting weight rankings.

(iii) The tensile strength of ECC significantly influences the load-carrying capacity of reinforced concrete beams, following a nonlinear relationship. A two-phase pattern is observed: minimal increase in load-carrying capacity at 2-7 MPa, followed by a steeper increase as tensile strength exceeds 7 MPa, reaching up to 14.5 MPa. Higher tensile strength improves the flexural performance of reinforced concrete beams by enhancing stress distribution and structural efficiency. These findings align with experimental studies, reinforcing the importance of ECC tensile strength in improving reinforced concrete beam performance.

(iv) ECC's strain capacity significantly improves the load-carrying capacity of reinforced concrete beams by enhancing ductility, toughness, and energy dissipation. Strain-hardening behavior allows ECC to endure higher strains, delaying failure and improving stress redistribution and resilience. The progressive cracking of ECC prevents brittle failure and maintains residual load capacity, especially beneficial in seismic design. ECC's superior bond with reinforcement optimizes load transfer, enhancing structural performance and prolonging the failure process. The influence of ECC's strain capacity is more pronounced in high-strength reinforced concrete beams, but the performance benefit becomes comparable at elevated strain levels in both beam types. Incorporating ECC into reinforced concrete beams leads to substantial improvements in load-carrying capacity with optimized design considerations for layer thickness and reinforcement type.

(v) ECC layer thickness positively influences the load-carrying capacity of reinforced concrete beams, with an almost linear relationship between thickness and load-carrying capacity. Thicker ECC layers enhance flexural stiffness, moment capacity, and tensile resistance, improving crack control and durability. In seismic scenarios, increased ECC thickness boosts energy dissipation, shear resistance, and crack bridging, especially in beams with inadequate shear reinforcement. Diminishing returns are observed beyond a certain ECC thickness, highlighting the existence of an optimal layer thickness for maximum benefit. Practical considerations, such as added weight, cost, and bond quality, must be considered when determining optimal ECC thickness for specific applications.

While the study provides a strong foundation for AI-driven predictive modeling, its findings are constrained by the quality and diversity of available data. Future research should focus on expanding the dataset, refining the neural network architecture, and exploring additional structural parameters to enhance the generalizability of the model.

Author's Contribuitions: The specific contributions of the authors to this manuscript are as follows: Conceptualization, A Tuken and YM Abbas; Methodology, YM Abbas; Investigation, A Tuken, YM Abbas, and NA Siddiqui; Writing - original draft, A Tuken, YM Abbas, and NA Siddiqui; Writing - review & editing, A Tuken, YM Abbas, and NA Siddiqui; Funding acquisition, YM Abbas and NA Siddiqui; Resources, YM Abbas and A Tuken; Supervision, YM Abbas.

Data Availability: The data that support the findings of this study are available from the corresponding author upon reasonable request.

Editor: Pablo Andrés Muñoz Rojas

References

Abbood, I. S., Rahman, N. A., & Abu Bakar, B. H. (2025). Enhanced data-driven shear strength predictive modeling framework for RCDBs using explainable boosting-based ensemble learning algorithms coupled with Bayesian optimization. *Results in Engineering*, *27*, 106556. https://doi.org/10.1016/j.rineng.2025.106556

Abbood, I. S., Rahman, N. A., & Bakar, B. H. A. (2025). Shear Strength Prediction for RCDBs Utilizing Data-Driven Machine Learning Approach: Enhanced CatBoost with SHAP and PDPs Analyses. *Applied System Innovation*, *8*(4), 96. https://doi.org/10.3390/asi8040096

Afefy, H. M., Kassem, N., & Hussein, M. (2015). Enhancement of flexural behaviour of CFRP-strengthened reinforced concrete beams using engineered cementitious composites transition layer. *Structure and Infrastructure Engineering*, *11*(8), 1042–1053. https://doi.org/10.1080/15732479.2014.930497

AFGC. (2002). *Bétons Fibrés à Ultra-hautes Performances*. Association Française du Génil Civil (AFGC).

Agliari, E., Albanese, L., Alemanno, F., Alessandrelli, A., Barra, A., Giannotti, F., Lotito, D., & Pedreschi, D. (2023). Dense Hebbian neural networks: A replica symmetric picture of unsupervised learning. *Physica A: Statistical Mechanics and Its Applications*, *627*, 129143. https://doi.org/10.1016/J.PHYSA.2023.129143

Ali, Y., & Khan, S. W. (2017). Experimental Study on the Flexural Behavior of Composite RC Beams having an Engineered Cementitious Composite Layer at the Bottom. *International Journal of Advances in Mechanical and Civil Engineering*, *4*(4), 44–49.

Arulanandam, P. M., Sivasubramnaian, M. V. R., Chellapandian, M., Murali, G., & Vatin, N. I. (2022). Analytical and Numerical Investigation of the Behavior of Engineered Cementitious Composite Members under Shear Loads. *Materials 2022, Vol. 15, Page 4640*, *15*(13), 4640. https://doi.org/10.3390/MA15134640

Asgari, M. A., Mastali, M., Dalvand, A., & Abdollahnejad, Z. (2019). Development of deflection hardening cementitious composites using glass fibres for flexural repairing/strengthening concrete beams: experimental and numerical

studies. *European Journal of Environmental and Civil Engineering*, *23*(8), 916–944. https://doi.org/10.1080/19648189.2017.1327888

Awad, F., Husain, M., & Fawzy, K. (2022). Flexural behaviour of reinforced concrete beams strengthened by NSM technique using ECC. *Frattura Ed Integrità Strutturale*, *16*(60), 291–309. https://doi.org/10.3221/IGF-ESIS.60.21

Basha, A., Fayed, S., & Elsamak, G. (2019). Flexural Behavior of Cracked RC Beams Retrofitted with Strain Hardening Cementitious Composites. *KSCE Journal of Civil Engineering*, *23*(6), 2644–2656. https://doi.org/10.1007/s12205-019-1874-4

Cahyati, M. D., Huang, W. H., & Hsu, H. L. (2021). Numerical modeling on varying patch repair size of cracked beam using engineered cementitious composites. *World Journal of Engineering*, *18*(1), 14–22. https://doi.org/10.1108/WJE-08-2019-0235/FULL/PDF

Daugevičius, M., Valivonis, J., Skuturna, T., & Popov, V. (2016). RC Beams strengthened with HPFRCC: Experimental and numerical results. *J. Civ. Eng. Manag.*, *22*(2), 254–270. https://doi.org/10.3846/13923730.2015.1124140

Emmanuel, T., Maupong, T., Mpoeleng, D., Semong, T., Mphago, B., & Tabona, O. (2021). A survey on missing data in machine learning. *Journal of Big Data*, *8*(1), 140. https://doi.org/10.1186/s40537-021-00516-9

fib Model Code for Concrete Structures. (2010). *fib – fédération internationale du béton / International Federation for Structural Concrete*. Ernst & Sohn GmbH & Co. KG.

Ge, W., Ashour, A. F., Cao, D., Lu, W., Gao, P., Yu, J., Ji, X., & Cai, C. (2019). Experimental study on flexural behavior of ECC-concrete composite beams reinforced with FRP bars. *Composite Structures*, *208*, 454–465. https://doi.org/10.1016/J.COMPSTRUCT.2018.10.026

Ge, W., Zhang, F., Wang, Y., Ashour, A., Luo, L., Qiu, L., Fu, S., & Cao, D. (2024). Machine learning predictions for bending capacity of ECC-concrete composite beams hybrid reinforced with steel and FRP bars. *Case Studies in Construction Materials*, *21*, e03670. https://doi.org/10.1016/J.CSCM.2024.E03670

Guo, X., Zhang, Z., Sun, Q., & Tian, P. (2024). Numerical Analysis on Flexural Shear Behavior of Reinforced Concrete Beams Strengthened with Fiber-Reinforced Polymer Grid and Engineered Cement Composites. *Buildings 2024, Vol. 14, Page 2304*, *14*(8), 2304. https://doi.org/10.3390/BUILDINGS14082304

Hemmati, A., Kheyroddin, A., & Sharbatdar, M. (2014). Proposed equations for estimating the flexural characteristics of reinforced HPFRCC beams. *Iranian Journal of Science and Technology. Transactions of Civil Engineering*, *38*(C2), 395.

Hossen, J., Ahmad, N., & Ali, S. M. (2017). An application of Pareto analysis and cause-and-effect diagram (CED) to examine stoppage losses: a textile case from Bangladesh. *The Journal of The Textile Institute*, *108*(11), 2013–2020. https://doi.org/10.1080/00405000.2017.1308786

Hu, Z., Zhou, Y., Hu, B., Huang, X., & Guo, M. (2022). Local use of ECC to simultaneously enhance the shear strength and deformability of RC beams. *Construction and Building Materials*, *353*, 129085. https://doi.org/10.1016/J.CONBUILDMAT.2022.129085

Hussein, M., Kunieda, M., & Nakamura, H. (2012). Strength and ductility of RC beams strengthened with steel-reinforced strain hardening cementitious composites. *Cement and Concrete Composites*, *34*(9), 1061–1066. https://doi.org/10.1016/j.cemconcomp.2012.06.004

Ibrahim, F. Q. (2021). Strengthen strategies for reinforced concrete haunched beams using fibre reinforced polymer fabric and engineered cementitious composites. *Periodicals of Engineering and Natural Sciences (PEN)*, *9*(3), 41. https://doi.org/10.21533/pen.v9i3.2076

Ismail, M. K., & Hassan, A. A. A. (2021). Structural performance of large-scale concrete beams reinforced with cementitious composite containing different fibers. *Structures*, *31*, 1207–1215. https://doi.org/10.1016/J.ISTRUC.2021.02.028

Ji, J., Zhang, Z., Lin, M., Li, L., Jiang, L., Ding, Y., & Yu, K. (2023). Structural application of engineered cementitious composites (ECC): A state-of-the-art review. *Construction and Building Materials*, *406*, 133289. https://doi.org/10.1016/J.CONBUILDMAT.2023.133289

Kamal, A., Kunieda, M., Ueda, N., & Nakamura, H. (2008). Assessment of strengthening effect on RC beams with UHP-SHCC. *Proc., Proceeding of JCI Annual Meeting, CD: File*, 1483–1488.

Khalil, A., Etman, E., Atta, A. , & Essam, M. (2017). Ductility Enhancement of Rc Beams Strengthened With Strain Hardening Cementitious Composites. *Proc. Int. Struct. Eng. Constr*, 1–6.

Khan, M. I., Fares, G., Abbas, Y. M., Abbass, W., & Sial, S. U. (2021). Susceptibility of strain-hardening cementitious composite to curing conditions as a retrofitting material for RC beams. *Journal of Engineered Fibers and Fabrics*, *16*, 155892502110203. https://doi.org/10.1177/15589250211020311

Khan, S. W., Ali, Y., Khan, F. A., Fahim, M., Gul, A., Ullah, Q. S., & Ul-Islam, S.-. (2023). Flexural Performance of Composite RC Beams Having an ECC Layer at the Tension Face. *Periodica Polytechnica Civil Engineering*. https://doi.org/10.3311/PPci.21017

Krishnaraja, A., & Kandasamy, S. (2017). Flexural performance of engineered cementitious composite-layered reinforced concrete beams. *Archives of Civil Engineering*, *63*(4), 173–189.

Krishnaraja, A. R., & Kandasamy, S. (2018). Flexural Performance of Hybrid Engineered Cementitious Composite Layered Reinforced Concrete Beams. *Periodica Polytechnica Civil Engineering*. https://doi.org/10.3311/PPci.11748

Kumar, K. L. V., & Karthikeyan, G. (2016). Experimental Study on Flexural response of Engineered Cementitious Composite (ECC) Strengthened Reinforced Concrete Beams. *International Journal of Advances in Engineering and Emerging Technology*, *7*(2), 84–91. https://erlibrary.org/erl/index.php/ijaeet/article/view/399

Li, H., Leung, C. K. Y., Xu, S., & Cao, Q. (2009). Potential use of strain hardening ECC in permanent formwork with small scale flexural beams. *Journal of Wuhan University of Technology-Mater. Sci. Ed.*, *24*(3), 482–487. https://doi.org/10.1007/s11595-009-3482-5

Liao, Q., Li, L., Li, B., & Yu, J. (2021). Prediction on the flexural deflection of ultra-high strength rebar reinforced ECC beams at service loads. *Structures*, *33*, 246–258. https://doi.org/10.1016/J.ISTRUC.2021.04.050

Liu, L., Yu, S., & Ma, X. (2023). Flexural capacity of RC beams reinforced with ECC layer and steel plate. *Journal of Building Engineering*, *65*, 105781. https://doi.org/10.1016/J.JOBE.2022.105781

Luković, M., Hordijk, D., Huang, Z., & Schlangen, E. (2019). Strain Hardening Cementitious Composite (SHCC) for crack width control in reinforced concrete beams. *Heron*, *64*(1/2), 181.

Naaman, A. E., & Wille, K. (2010, July). Some correlation between high packing density, ultra-high performance, flow ability, and fiber reinforcement of a concrete matrix. *BAC20102nd Iberian Congress on Self Compacting Concrete*.

Nguyen, D.-L., Tran, V.-T., Tran, N.-T., Ngo, T.-T., & Nguyen, M.-T. (2021). Evaluating Load-Carrying Capacity of Short Composite Beam Using Strain-Hardening HPFRC. *KSCE Journal of Civil Engineering*, *25*(4), 1410–1423. https://doi.org/10.1007/s12205-021-1327-8

O. El-Mahdy, O., A. Hamdy, G., H. El-Diasity, M., & Shalaby, Y. (2022). Performance of Reinforced Engineered Cementitious Composite Beams. *Engineering Research Journal - Faculty of Engineering (Shoubra)*, *51*(2), 83–101. https://doi.org/10.21608/erjsh.2022.235468

Qi, Z., Huang, Z., Li, H., & Chen, W. (2018). Study of Flexural Response in Strain Hardening Cementitious Composites Based on Proposed Parametric Model. *Materials 2019, Vol. 12, Page 113*, *12*(1), 113. https://doi.org/10.3390/MA12010113

Qin, F., Zhang, Z., Yin, Z., Di, J., Xu, L., & Xu, X. (2020). Use of high strength, high ductility engineered cementitious composites (ECC) to enhance the flexural performance of reinforced concrete beams. *Journal of Building Engineering*, *32*, 101746. https://doi.org/10.1016/j.jobe.2020.101746

Rizo-Maestre, C., Dolores Andújar-Montoya, M., Sempere-Tortosa, M. L., Emara, M., El-Zohairy, A., Fekry, M., & Husain, M. (2022). Effect of Using ECC Layer on the Flexural Performance of RC Beams Previously Strengthened with EB CFRP Laminates. *Sustainability 2022, Vol. 14, Page 16990*, *14*(24), 16990. https://doi.org/10.3390/SU142416990

Saranya, K., & Doraikkannan, J. (2018). Experimental Study on Flexural Response of ECC Strengthened Reinforced Concrete Beams. *International Journal for Scientific Research & Development*, *6*(1), 35–44.

Shanour, A. S., Said, M., Arafa, A. I., & Maher, A. (2018). Flexural performance of concrete beams containing engineered cementitious composites. *Construction and Building Materials*, *180*, 23–34. https://doi.org/10.1016/j.conbuildmat.2018.05.238

Shriram, J., Sreenath, S., & Saravana Raja Mohan, K. (2018). Strengthening of Reinforced Concrete Beams Using Engineered Cementitious Composites. *International Journal of Civil Engineering and Technology*, *9*, 608–613.

Siva, C. R., & Pankaj, A. (n.d.). Flexural behavior of reinforced concrete beams with high performance fiber reinforced cementitious composites. *Journal of Central South University*, *26*(9), 2609–2622.

Skazlic M, Bjegovic D, & Serdar M. (2008). Influence of test specimen's geometry on compressive strength of ultra-high-performance concrete. *The 2nd International Symposium on Ultra-High-Performance Concrete*, 295–301.

Tabrizikahou, A., Kuczma, M., Łasecka-Plura, M., & Noroozinejad Farsangi, E. (2022). Cyclic Behavior of Masonry Shear Walls Retrofitted with Engineered Cementitious Composite and Pseudoelastic Shape Memory Alloy. *Sensors*, *22*(2), 511. https://doi.org/10.3390/s22020511

Tuken, A., Abbas, Y. M., & Siddiqui, N. A. (2023). Efficient prediction of the load-carrying capacity of ECC-strengthened RC beams – An extra-gradient boosting machine learning method. *Structures*, *56*, 105053. https://doi.org/10.1016/J.ISTRUC.2023.105053

Umer Sial, S., & Iqbal Khan, M. (2018). Performance of Strain hardening cementitious composite as strengthening and protective overlay in flexural members. *MATEC Web of Conferences*, *199*, 09005. https://doi.org/10.1051/matecconf/201819909005

Wang, C., Sun, R., Hu, X., Guan, Y., Yang, Y., Lu, W., Tian, J., Zhang, H., Ge, Z., & Šavija, B. (2023). Chloride penetration resistance of engineered cementitious composite (ECC) subjected to sustained flexural loading. *Materials Today Communications*, *35*, 106080. https://doi.org/10.1016/J.MTCOMM.2023.106080

Wang, G., Yang, C., Pan, Y., Zhu, F., Jin, K., Li, K., & Nanni, A. (2019). Shear Behaviors of RC Beams Externally Strengthened with Engineered Cementitious Composite Layers. *Materials*, *12*(13), 2163. https://doi.org/10.3390/ma12132163

Wang, G., Zhu, F., & Yang, C. (2020). Experimental study on Shear behaviors of RC beams strengthened with ECC layers. *IOP Conference Series: Materials Science and Engineering*, *780*(4), 042024. https://doi.org/10.1088/1757-899X/780/4/042024

Wei, J., Wu, C., Chen, Y., & Leung, C. K. Y. (2020). Shear strengthening of reinforced concrete beams with high strength strain-hardening cementitious composites (HS-SHCC). *Materials and Structures*, *53*(4), 102. https://doi.org/10.1617/s11527-020-01537-1

Wu, Q., You, J., Wang, H., Wan, D., Hou, Z., Li, Y., Wang, Y., Chen, X., & Liu, L. (2024). Flexural behavior of over-reinforced beam with ECC layer: Experimental and numerical simulation study. *Heliyon*, *10*(19). https://doi.org/10.1016/j.heliyon.2024.e38271

Yuan, F., Chen, M., & Pan, J. (2020). Flexural strengthening of reinforced concrete beams with high-strength steel wire and engineered cementitious composites. *Construction and Building Materials*, *254*, 119284. https://doi.org/10.1016/J.CONBUILDMAT.2020.119284

Zhang, Y. (2018). Flexural Behavior Investigation of Reinforced Concrete Member with Strengthening Using Strain Hardening Cementitious Composite. *International Journal of Civil Engineering*, *16*(7), 837–843. https://doi.org/10.1007/S40999-017-0220-9/FIGURES/9

Zhao, D., Li, K., Fan, J., Wang, Y., & Zhu, J. (2024). Shear behavior of RC beams strengthened with high-strength steel strand mesh reinforced ECC: Shear capacity, cracking and deformation. *Engineering Structures*, *298*, 117081. https://doi.org/10.1016/J.ENGSTRUCT.2023.117081

Zhu, J. X., Xu, L. Y., Huang, B. T., Weng, K. F., & Dai, J. G. (2022). Recent developments in Engineered/Strain-Hardening Cementitious Composites (ECC/SHCC) with high and ultra-high strength. *Construction and Building Materials*, *342*, 127956. https://doi.org/10.1016/J.CONBUILDMAT.2022.127956